Dissociation energies of six NO_2 isotopologues by laser induced fluorescence spectroscopy and zero point energy of some triatomic molecules

G. Michalski
University of California, San Diego, La Jolla, California 92093-0356

R. Jost, D. Sugny, and M. Joyeux
*Laboratoire Spectrometrie Physique, CNRS UMR 5588, Université Joseph Fourier-Grenoble I,
Boite Postale 87, 38402 St. Martin d'Heres Cedex, France*

M. Thiemens
University of California, San Diego, La Jolla, California 92093-0356

We have measured the rotationless photodissociation threshold of six isotopologues of NO_2 containing ^{14}N, ^{15}N, ^{16}O, and ^{18}O isotopes using laser induced fluorescence detection and jet cooled NO_2 (to avoid rotational congestion). For each isotopologue, the spectrum is very dense below the dissociation energy while fluorescence disappears abruptly above it. The six dissociation energies ranged from 25 128.56 cm^{-1} for $^{14}N^{16}O_2$ to 25 171.80 cm^{-1} for $^{15}N^{18}O_2$. The zero point energy for the NO_2 isotopologues was determined from experimental vibrational energies, application of the Dunham expansion, and from canonical perturbation theory using several potential energy surfaces. Using the experimentally determined dissociation energies and the calculated zero point energies of the parent NO_2 isotopologue and of the NO product(s) we determined that there is a common $D_e = 26\,051.17 \pm 0.70$ cm^{-1} using the Born-Oppenheimer approximation. The canonical perturbation theory was then used to calculate the zero point energy of all stable isotopologues of SO_2, CO_2, and O_3, which are compared with previous determinations. © *2004 American Institute of Physics.* [DOI: 10.1063/1.1792233]

I. INTRODUCTION

Stable isotopes have a rich history of applications in chemical physics, biogeochemistry, and cosmochemistry. The observed shift in vibrational frequencies between a molecule and its isotopologues was utilized in early spectroscopy to obtain accurate force constants and bond angles.[1] Urey[2] and Bigeleisen and Mayer[3] pioneered the theoretical basis for determining the differences in the thermodynamic and kinetic properties of isotopologues through the use of the isotopic reduced partition function. The temperature dependence of these differences results in isotopic compositions that are utilized as geochemical thermometers, biochemical tracers, and the ability to constrain budgets in biogeochemical systems.[4] The calculation of the partition function relies on approximations, specifically ignoring the electronic partition function and application of the harmonic oscillator and rigid rotor approximation models. These calculations assume the validity of the Born-Oppenheimer (BO) approximation and make predictions about the zero point energy (ZPE) for isotopically substituted molecules and their relative differences (ΔZPE).

The shift of the ZPE between isotopologues is not directly accessible experimentally; rather they are derived from model dependent extrapolations of spectroscopic data (e.g., Dunham expansions). In contrast, for a few molecules, particularly NO_2, the dissociation energy D_0 can be precisely measured and its isotopologue shift (ΔD_0) may be obtained for its isotopologues. In the Born-Oppenheimer limit, ΔD_0 is equal to the difference of the ΔZPEs of the parent (NO_2) and product (NO) molecules (see below). Therefore, ΔD_0 is a direct test of the BO approximation at high energies and an accurate measurement of ZPE if this limit is realized. In addition, precise D_0 and ΔZPE values are important for calculating the isotopic effect in photodissociation processes on Earth and other planetary atmospheres.[5,6]

Shifts in ZPE and non-Ramsperger, Rice, Kassel, and Marcus (RRKM) density of states distributions have recently been suggested as the source of mass-independent isotopic fractionations (MIF) that are known to occur during the formation of ozone.[7–10] These observed mass-independent fractionations show approximately equal enrichments of ^{17}O and ^{18}O where the standard theory based on partition function ratios predicts that ^{17}O fractionations should be approximately half of those in ^{18}O when normalized to ^{16}O.[11] Recent theoretical studies on MIF mechanisms have suggested that the reduction of symmetry upon isotopic substitution is the root cause of the effect.[8] For C_{2v} triatomic molecules such as O_3, NO_2, SO_2, the reduction of symmetry from C_{2v} to C_6 by a single oxygen isotopic substitution must be considered from both the energetic and dynamical points of view. The energetic aspect is related to the energy splitting, ΔZPE, between the two different dissociation channels, e.g., $^{18}O^{16}O^{16}O \rightarrow {}^{18}O^{16}O + {}^{16}O$ and $^{16}O^{16}O + {}^{18}O$ for which ΔZPE ≈ 22 cm^{-1}. In this energy gap of ΔZPE, only one exit channel is energetically open and should not result in a MIF

effect since the ^{17}O isomers will have ΔZPE shifted by half as much. However, in the case of ozone, recent *ab initio* calculations have predicted that long lived resonances may exist in the energy gap of ΔZPE leading to anomalous isotopic distributions.[9] The dynamical aspect is related to the density of rovibrational levels $[\rho(E)]$, a key parameter in RRKM theory. It has been suggested that $\rho(E)$ may be larger for the asymmetric isotopologues[8] providing the excited state asymmetric ozone a longer predissociative lifetime and enhanced quenching to ground state ozone. Since symmetry is broken by either ^{17}O or ^{18}O the enrichment is approximately equal. These studies also emphasized the importance of exit channel energies that are directly related to ΔZPE and that the existence of two different exit channels in asymmetric isotopologues is the key to the observed overall isotopic enrichment when conventional theory predicts overall depletion.[12,13] However, there has been no direct experimental test of either ΔZPE or $\rho(E)$ in ozone at the dissociation threshold; rather they are derived from the culmination of experimental data on isotopic effects observed during the formation of ozone (see reviews by Thiemens[14] and Mauersberger[15]).

For ozone, it is difficult to spectroscopically assess ΔZPE and $\rho(E)$, using enriched $^{18}O_2$, for two reasons. First, because of O atom exchange with O_2, which occurs $\sim 10^3$ faster than O_3 formation,[16] four symmetric and two asymmetric isotopomers are produced. Thus, spectroscopic analysis of rovibronic density is unattainable due to spectral congestion. Second, direct ozone dissociation is not observed at the D_0 threshold but only via predissociation, i.e., through a barrier. NO_2 is another C_{2v} molecule whose symmetry can be isotopically reduced to C_s and should simulate the anomalous isotopic compositions observed in ozone.[8] Large mass independent compositions have been observed in atmospheric HNO_3 (the main sink of NO_2), but have been attributed to O atom transfer mechanisms during oxidation by ozone.[17] This model assumes that there is no fundamental MIF process occurring during NO_2 photochemistry. Isotopic studies on the photodissociation dynamics of NO_2 isotopologues are significant as NO_2 is a prototype C_{2v} molecule that may be used to test current MIF theoretical predictions of non-RRKM density distributions. In addition, isotopic effects arising from ΔZPE or dissociation dynamics are important for understanding mass dependent isotopic fractionations in NO_2 and their applications in biogeochemical systems involving NO_x.

NO_2 is highly amendable to spectroscopic studies because of its fluorescence properties up to D_0.[18–20] NO_2 fluorescence occurs in the visible spectral region for the electronic transitions from the $A\,^2B_2$ state back to the $X\,^2A_1$ state. The $X\,^2A_1$ ground state has maximum Franck-Condon overlap with the $A\,^2B_2$ state around 3 eV, which, by chance, is close to D_0 at 25 128.56 cm^{-1} (3.115 eV). The eigenstates observed by optical excitation are not fully assignable above $\sim 12\,000$ cm^{-1} (Ref. 21) because of a conical intersection between the $A\,^2B_2$ and $X\,^2A_1$ potential energy surface (PES) that promotes vibronic mixing between the two states. This leads to vibronic chaos above $\sim 16\,000$ cm^{-1} (Ref. 22) and by $\sim 24\,000$ cm^{-1} only the total angular momentum quantum

number J can be determined because rovibronic mixing has become extensive.[18] This mixing has been described as rovibronic chaos. Nonetheless, most of the rovibronic eigenstates located near D_0 can be detected experimentally, and the direct determination of D_0 and the density of states up to D_0 is experimentally possible because modern techniques provide spectral resolutions of 0.005 cm^{-1}.[18]

These characteristics make NO_2 the ideal molecule to test some of the recent MIF theories and also to numerically verify the accuracy of the Born-Oppenheimer approximation with respect to classical isotopic fractionation models for molecules with low lying electronic states. Here we present the precise determination of D_0 for six isotopologues of NO_2 using jet cooled laser induced fluorescence (LIF). Then, we relate the variations of D_0 (ΔD_0) to the shifts in the ZPE (ΔZPE) of NO_2 and of the NO products by assuming that the Born-Oppenheimer approximation is valid. We also compare the ZPE and ΔZPE obtained by two methods, namely, the anharmonic Dunham expansion and canonical perturbation theory (CPT).[23] The CPT method is then used to determine the ZPE of all isotopologues of several triatomic molecules important in atmospheric chemistry: O_3, SO_2, and CO_2. In a forthcoming paper we will address the effect that symmetry has on the density of states near D_0 for the NO_2 molecule and its relevance to current MIF theory.

II. EXPERIMENT

The LIF experimental setup has been detailed previously.[24] Briefly, an Ar^+ pump laser (Spectra Physics) generates ≈ 15 W of 512 and 488 nm light that is used to excite a tunable, monomode, cw Ti:sapphire laser (Coherent 899). The Ti:sapphire crystal lases and generates a spectrum of light spanning ~ 700–1000 nm, which can be tuned using two etalons and one Lyot filter (three plates) to a spectral width of few megahertz with an output power of ~ 2 W. A small portion of the beam is split and passed through both a Fabry-Perot etalon and a 1 m iodine cell (at 800 K). The etalon is used to check and calibrate scan linearity, while a custom-built 8-digit lambdameter is used to measure wavelengths to within 150 MHz (relative) and 500 MHz (absolute). The iodine cell refines the calibration of the absolute energy scale using the known I_2 spectral atlas for energies between 11 000 and 14 000 cm^{-1}. The main portion of the tuned beam is then frequency doubled using a lithium diborate (LBO) doubling crystal (doubler: laser analytic systems) giving an output beam spanning 380–410 nm with few megahertz of linewidth and an intensity up to ~ 200 mW. The doubled beam is directed through a jet expansion chamber whose internal pressure is maintained at $\sim 10^{-2}$ Torr using two root pumps (1000 and 250 m^3/b) and a mechanical pump.

A 1% mixture of NO_2 in a He carrier gas is injected into the chamber through a 100 μm pinhole jet with a back pressure of 3 bars. The gas passes through a pinhole jet and undergoes supersonic expansion that rotationally cools the NO_2 down to ~ 1 K. The laser beam intersects the molecular jet ≈ 3 mm after the pinhole. This produces a fluorescence "flame," the length of which depends on the lifetime of the excited level. This flame is imaged out of the chamber and

screened with a narrow observation slit, ≈ 300 μm in width and 4 mm long, and detected using a photomultiplier tube. This slit allows one to observe only the excited molecules, which travel perpendicular to the laser beam and for which the Doppler shift effect is zero. The flame width and the slit adjustments allow a residual Doppler width of ~ 0.005 cm^{-1}.

Among the isotopologues of interest, only $^{14}N^{16}O_2$ and $^{15}N^{16}O_2$ are commercially available and both isotopologues were used with no further purification. The other isotopologues were synthesized in a Pyrex vacuum/purification line as described below. $^{14}N^{18}O_2$ was produced by mixing high purity $^{14}N_2$ (99.99%, Airgas) and 99% pure $^{18}O_2$ (Sigma-Aldrich) in a 1:15 ratio at a total pressure of 100 Torr. A recirculation pump flowed the gas mixture in a circular path that ultimately passed between two wire electrodes powered by a Tesla coil. The electrodes generated a N and O plasma in which the ions recombine to form small amounts of NO_x (NO+NO$_2$) that was collected as N_2O_3 (noted by its characteristic blue color) using a liquid nitrogen trap. Excess $^{18}O_2$ was then added to the system, the N_2O_3 trap was thawed, and the gases were allowed to react ($2N_2O_3 + O_2 \rightarrow 4NO_2$). NO$_2$ was then cryogenically isolated and the procedure repeated until about 1 l at 1 atm of $^{14}N^{18}O_2$ was produced. $^{16}O^{14}N^{18}O$ was produced by mixing 99% pure $^{18}O_2$ with $^{14}N^{16}O$ and waiting ~ 20 min for the 2NO+O$_2$ $\rightarrow 2$ NO$_2$ reaction to occur. The NO$_2$ was repeatedly distilled at 220 K until only a pure white solid remained. Several studies have indicated that this reaction results in the formation of the predominantly asymmetric NO$_2$ molecules. Our results show that isotopic scrambling occurs rather quickly, so that this procedure resulted in a NO$_2$ mixture containing all three possible $^{14}N/^{16,18}O$ isotopologues. The same procedure was carried out using $^{15}N^{16}O$ (98% pure, Sigma-Aldrich) and $^{18}O_2$ (99% pure, Sigma-Aldrich) to generate a mixture of the three $^{15}N/^{16,18}O$ isotopologues, including $^{15}N^{18}O_2$. An aliquot ($\sim 1/3$) of each NO$_2$ isotopologue was retained to be used in future high-resolution Fourier transform infrared studies. All NO$_2$ isotopologues were kept in precleaned glass vials and stored in the dark prior to analysis.

Prior to each LIF experiment one of the isotopologues was transferred to a high-pressure stainless steel tank and high purity He (99.99% pure) was added to a total pressure of ~ 30 bars. Because pure, rare isotope gases are expensive and only available in limited quantities we added a cryogenic trap (77 K) just ahead of the root pump outlet attached to the laser vacuum chamber in order to trap the residual NO$_2$ gas. A secondary collection system was added in parallel to the main trap to collect the NO$_2$ for reuse without exposing the vacuum chamber to the atmosphere. The liquid nitrogen trap installed after the expansion cavity recovered >90% of the NO$_2$ flux with minor contamination of the oxygen isotopes from either H$_2$O absorbed on the metal surface or from residual NO$_2$ from previous runs, allowing for multiple analysis of each isotopologue.

III. EXPERIMENTAL DISSOCIATION ENERGIES (D_0) OF SIX 6 NO$_2$ ISOTOPOLOGUES

The NO$_2$ dissociation energy threshold (D_0) corresponds, experimentally, to the abrupt disappearance of the
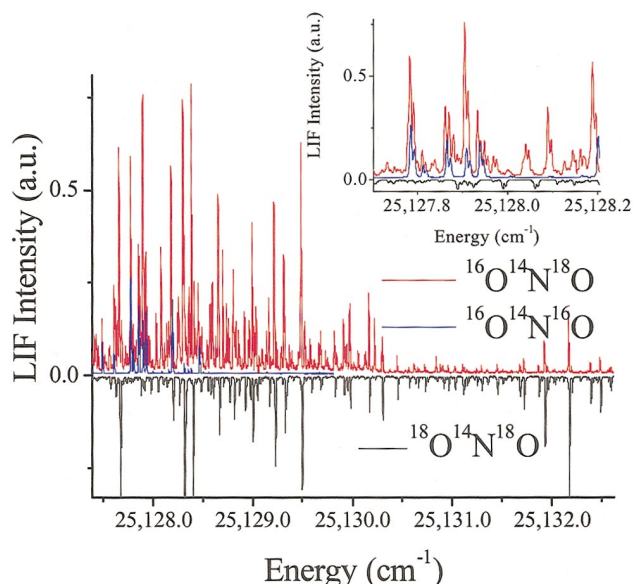

FIG. 1. (Color) Overlay of the LIF spectra of $^{14}N^{18}O_2$ (black, negative intensity), $^{14}N^{16}O_2$ (blue), and $^{16}O^{14}N^{18}O$ (red). Inset is an expansion of the region below D_0 of $^{14}N^{16}O_2$ and shows that $^{16}O^{14}N^{18}O$ spectra contain excitation lines from all three ^{14}N isotopologues.

NO$_2$ fluorescence when the photon energy increases to energies above D_0.[18] Correlatively, just above D_0, it has been shown that LIF signals of the dissociation products, the NO molecule and oxygen atom, appear.[19,25] The fluorescence spectrum for the ^{14}N isotopologues of NO$_2$ ($^{14}N^{16}O_2$, $^{14}N^{18}O_2$, and $^{16}O^{14}N^{18}O$) near D_0 is shown in Fig. 1. The $^{14}N^{16}O_2$ sample shows clear fluorescence up to about 25 128.56 cm^{-1} where dissociation into NO($^2\Pi_{1/2}$) + O($^3P_2$) occurs.[18,25] The LIF spectrum of the $^{16}O^{14}N^{18}O$ sample is extremely dense up to about 25 130.3 cm^{-1}, after which both line density and fluorescence intensity are greatly reduced. In addition, for energies above 25 130.3 cm^{-1} there is a one-to-one correlation between the fluorescence lines of the sample containing $^{16}O^{14}N^{18}O$ and those of the $^{14}N^{18}O_2$ sample up to the latter's dissociation threshold (see below).

From these spectra, it is clear that our various NO$_2$ isotopologue samples are not pure because of two reasons: First, because scrambling of oxygen atoms from self-exchange occurs during formation of the N_2O_4 dimer, and, second, because of isotopic contamination of our "pure" gases. This is evident when examining closely the region of the $^{14}N^{16}O_2$ spectra below D_0, with the $^{16}O^{14}N^{18}O$ spectra superimposed (inset of Fig. 1). The spectra show that there are also coincident lines with exactly the same excitation energy. It is clear that after the synthesis of the asymmetric isotopologue complete isotopic scrambling occurred so that the asymmetric $^{16}O^{14}N^{18}O$ sample actually contains all three possible $^{14}N/^{16,18}O$ isotopologues. Isotopic scrambling was also observed in the $^{15}N/^{16,18}O$ isotopologues spectra. Therefore, in order to spectroscopically establish D_0 of the two asymmetric isotopologues the spectral resolution and energy scale must be of sufficient precision to allow subtraction of the symmetric isotopologues spectra's from those of the mixed gas containing the asymmetric species. Similar difficulties arose from contamination of a few percent of light

TABLE I. The D_0 energies from this study, the ZPE of NO isotopologues derived from spectroscopic data (Refs. 34 and 35), and the ZPE of NO_2 derived from spectroscopic data (ZPE_{Dun}) (Ref. 41) and GF calculations and from CPT calculations ($ZPE_{CPT-Resc}$) using the PES of Ref. 43. Dissociation energies (D_e) using either ZPE from Dunham coefficients ($D_{e\ Dun}$) or ZPE from CPT ($D_{e\ CPT-Resc}$) are calculated using Eq. (1). $\langle D_{e\ Dun} \rangle = 26051.28 \pm 0.44$ cm^{-1}; $\langle D_{e\ CPT-Resc} \rangle = 26051.22 \pm 0.36$ cm^{-1}.

	$^{14}N^{16}O_2$	$^{14}N^{18}O_2$	$^{15}N^{16}O_2$	$^{15}N^{18}O_2$	$^{16}O^{14}N^{18}O$	$^{16}O^{15}N^{18}O$
D_0 (this study)	25 128.56	25 158.70	25 141.50	25 171.80	25 130.92	25 143.86
ZPE_{NO}[a]	948.53	923.58	931.64	906.29	923.58	906.29
ZPE_{Dun}	1871.05[b]	1816.60	1841.26	1785.88	1843.95	1813.54
$ZPE_{CPT-Resc}$[c]	1871.05 (ref)	1816.43	1841.06	1785.82	1843.91	1813.63
$D_{e\ Dun}$	26 051.08	26 051.72	26 051.12	26 051.39	26 051.29	26 051.11
$D_{e\ CPT-Resc}$	26 051.08 (ref)	26 051.55	26 050.92	26 051.33	26 051.25	26 051.20
Diff from $^{14}N^{16}O_2$	0.00 (ref)	0.47	−0.16	0.25	0.17	0.12

[a]References 34 and 35.
[b]Reference 41.
[c]Reference 43.

isotopes in our enriched gases; however these also could be resolved using intensity changes and correlations with energy at high spectral resolution. The determination of the D_0 energies (summarized in Table I) presented in the following sections will consider the symmetric isotopologues first, as these are the least ambiguous. The excitation lines caused by isotope contamination in the enriched samples (or natural abundance in $^{14}N^{16}O_2$) are very minor in intensity for these spectra. After establishing these D_0 energies, the more complex asymmetric isotopologues D_0 energies will be attained by peak subtractions from complex spectra.

A. D_0 of symmetric isotopologues $^{14}N^{18}O_2$, $^{14}N^{16}O_2$, $^{15}N^{18}O_2$, and $^{15}N^{16}O_2$

The LIF spectrum of the $^{14}N^{18}O_2$ isotopologue in the last $\sim$3 cm^{-1} below D_0 is typical of the spectral resolution for the enriched symmetric isotopologues (Fig. 2). The D_0 of $^{14}N^{18}O_2$ has been precisely determined at $25\,158.70 \pm 0.03$ cm^{-1} with the minor lines above 25 158.70 cm^{-1} attributed to fluorescence by the $^{15}N^{18}O_2$ isotopologue, the only NO_2 isotopologue expected to have a greater D_0 than $^{14}N^{18}O_2$. We have reflected the $^{15}N^{18}O_2$ spectrum on the same energy and relative intensity scales as $^{14}N^{18}O_2$ in the inset of Fig. 2 (note the artificial enhancement of the $^{14}N^{18}O_2$ lines by a

factor of 100). There is a clear one-to-one correspondence between strong fluorescence lines in the $^{15}N^{18}O_2$ spectra and weak lines occurring after the last strong fluorescence line at 25 158.70 cm^{-1} in the $^{14}N^{18}O_2$ gas, confirming that these minor lines are indeed from trace amounts of $^{15}N^{18}O_2$.

The $^{14}N^{18}O_2$ spectra become less congested in the final $\sim$2.3 cm^{-1} where only the R_0 lines remain, as previously observed for the $^{14}N^{16}O_2$ isotopologue. The first clearly assignable P_2 line is located at 25 156.06 cm^{-1}, with two possible P_2 lines at 25 156.21 and 25 156.41 cm^{-1}. However, these latter two lines are of low intensity and on the shoulder of larger R_0 lines and absolute determination of their assignment is tenuous. The 25 156.41 cm^{-1} P_2 line would correspond to a 2.24 cm^{-1} shift from the corresponding R_0 line at 25 158.65 cm^{-1}. This is in agreement with 6 B=2.25 cm^{-1}, the difference between the $N=2$, $K=0$ and the $N=0$, $K=0$ of the $^{14}N^{18}O_2$ ground state, B being measured at 0.375 cm^{-1} by Brand, Chan, and Hardwick.[26]

The determination of D_0 for the $^{14}N^{16}O_2$ isotopologue at $25\,128.56 \pm 0.03$ cm^{-1} (Fig. 3) is in excellent agreement with the previously published value (25 128.57 cm^{-1}).[18,19] The 0.01 cm^{-1} difference is not the result of experimental uncertainty but rather it was determined that the last minor line in the cluster beginning at 25 128.50 [see Jost *et al.* (1996)] belongs to the $^{15}N^{16}O_2$ isotopologue. Several other very weak lines observed beyond D_0 of $^{14}N^{16}O_2$ have been suspected as being the result of trace of other isotopologues. A comparison between the $^{14}N^{16}O_2$ and $^{15}N^{16}O_2$ spectra above 25 128.0 cm^{-1} shows a direct energy correspondence be-
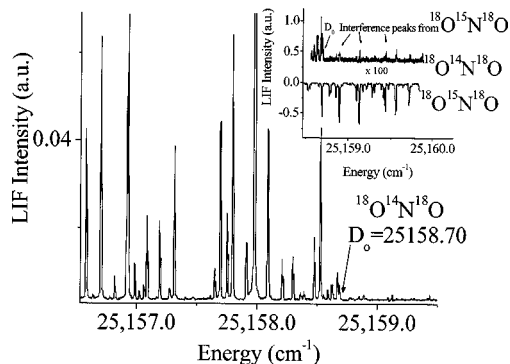

FIG. 2. D_0 of the $^{14}N^{18}O_2$ isotopologue with inset showing the minute lines originating from trace contamination of the $^{15}N^{18}O_2$ isotopologue.
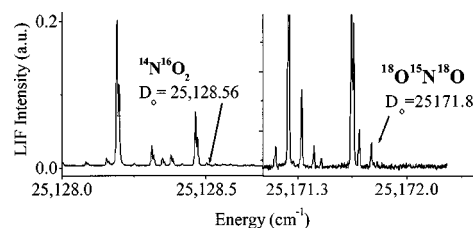

FIG. 3. D_0 of the $^{14}N^{16}O_2$ and $^{15}N^{18}O_2$ isotopologues.

tween these minor lines and strong lines in the $^{15}N^{16}O_2$ spectra, with a intensity ratio in good agreement with the known natural abundance of ^{15}N (0.3%). These lines were confirmed to be due to $^{15}N^{16}O_2$ by observing the difference in the line shape due to the hyperfine splitting in the $N=0$ ground state, which is different for the ^{14}N and ^{15}N isotopologues. As was observed in previous studies of the $^{14}N^{16}O_2$ isotopologue the fluorescence transitions below $\sim D_0 - 0.5\,cm^{-1}$ are congested, irregular, and unassignable using vibrational or rotational quantum numbers.[22,27] In addition, the region below $(D_0 - 2.53\,cm^{-1})$ has three types of rotational transitions because P_2 and R_2 lines can be detected in addition to the R_0 lines that are observed up to D_0. The energy shift of 2.53 cm^{-1} between the two thresholds corresponds to 6 B, which is the rotational energy of the $N=2$ $(K=0)$ rotational level of the $^2A_1$ (0,0,0) vibrational level (the ground state). Note that odd N does not exist in the ground states of $^{14}N^{16}O_2$, $^{14}N^{18}O_2$, $^{15}N^{16}O_2$, and $^{15}N^{18}O_2$.

Determination of the D_0 of the $^{15}N^{18}O_2$ isotopologue is not made more difficult by the isobaric lines observed in the $^{14}N^{16}O_2$ and $^{14}N^{18}O_2$ isotopologues, because it contains all heavy isotopes producing the highest D_0 as a result of its zero point energy being the lowest one in the $X\,^2A_1$ potential energy well. Therefore, any fluorescence line due to traces of the more abundant light isotopes of N and O would be below the dissociation region. We could not obtain the isotopically enriched gases to synthesize the $^{15}N^{18}O_2$ isotopologue, so our ability to determine its D_0 is a fortuitous result of isotopic scrambling. The reduced signal to noise ratio in the $^{15}N^{18}O_2$ spectra (Fig. 3) is due to the decrease in concentration of this isotopologue relative to that in a pure sample (statistically only $\sim 25\%$ of the scrambled gas is expected to be $^{15}N^{18}O_2$). The $^{15}N^{18}O_2$ D_0 is found at 25 171.80 cm^{-1} (Fig. 3), with the line shape of the $^{15}N^{18}O_2$ R_0 lines reversed relative to the ^{14}N isotopologues. This is due to the difference in nuclear spin of the nitrogen isotopes, where $I=\frac{1}{2}$ for ^{14}N and $I=1$ for ^{15}N as discussed above. Note that hyperfine splitting and line intensities have been calculated by Persch, Vedder, and Demtroeder only for the ^{14}N isotope.[28]

In the LIF spectrum of the $^{15}N^{16}O_2$ sample there was evidence of a significant contribution of $^{18}O(\sim 10\%)$, mainly as $^{16}O^{15}N^{18}O$, but with a trace amount of $^{15}N^{18}O_2$. This assignment required subtracting out the asymmetric isotopologue, $^{16}O^{15}N^{18}O(\sim 10\%)$, and symmetric $^{15}N^{18}O_2$ isotopologue $(<1\%)$ spectra. The same subtraction was required for determining the D_0 of $^{16}O^{14}N^{18}O$ and $^{16}O^{15}N^{18}O$. The spectral stripping process will be discussed in the following section, but the spectral resolution in sum leads to the assignment of D_0 of $^{15}N^{16}O_2$ at 25 141.50 cm^{-1}, $\pm 0.05\,cm^{-1}$.

B. D_0 of asymmetric isotopologues $^{16}O^{14}N^{18}O$ and $^{16}O^{15}N^{18}O$

Due to the oxygen exchange (or "scrambling"), the analysis of the nominal $^{16}O^{14}N^{18}O$ spectra requires a comparison of spectra from samples with different oxygen isotope ratios. Figure 1 shows that, for energies higher than the $^{14}N^{16}O_2$ D_0 limit (25 128.56 cm^{-1}), the scrambled $^{14}N/^{16,18}O$ spectra remain dense and intense up to $\approx 25\,130.2\,cm^{-1}$ after
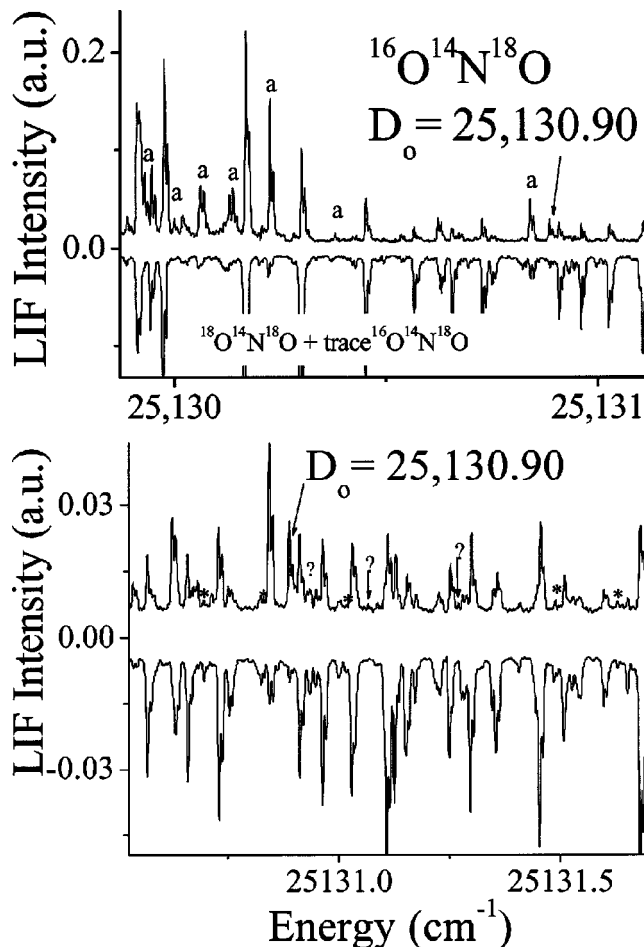

FIG. 4. (i) LIF of $^{16}O^{14}N^{18}O$ isotopologue (positive intensity) and $^{14}N^{18}O_2$ isotopologue negative intensity) near D_0. The final, definitive, excitation lines of the $^{16}O^{14}N^{18}O$ isotopologue at D_0 (a) and also contains trace amounts of $^{14}N^{18}O_2$. Possible $^{16}O^{14}N^{18}O$ lines lying above the theoretical D_0 are evident (?). (ii) An expansion of the energy range containing these spurious lines shows three to four possible fluorescence lines above the expected D_0 of $^{16}O^{14}N^{18}O$ indicating possible long lived resonances for the asymmetric isotopologue.

which the intensities dramatically drop. Above 25 130.2 cm^{-1} there is a one-to-one correlation, with a fluorescence intensity ratio of $\sim 1:3$, between the two spectra from samples containing dominantly either $^{16}O^{14}N^{18}O$ or $^{14}N^{18}O_2$. An expansion of this region between 25 128.0 and 25 130.5 cm^{-1} is shown in Fig. 4. Since this is above the $^{14}N^{16}O_2$ D_0 threshold and ^{15}N has already been shown to be $<1\%$, only the fluorescence interferences between the $^{16}O^{14}N^{18}O$ and $^{14}N^{18}O_2$ isotopologues are considered. Two correlations are observed. The first are those lines in the scrambled gas (labeled a) that correspond to lines of $^{16}O^{14}N^{18}O$ in the nominal $^{14}N^{18}O_2$ sample spectra and exhibit an intensity ratio $\sim 10:1$. The second correlation is between those lines in the $^{14}N^{18}O_2$ spectra that are reflected in the scrambled gas with an intensity ratio of $\sim 1:5$. This is evidence that the nominal $^{16}O^{14}N^{18}O$ sample has appreciable $^{14}N^{18}O_2$ and that the nominal $^{14}N^{18}O_2$ sample contains several percent of $^{16}O^{14}N^{18}O$. The D_0 of $^{16}O^{14}N^{18}O$ is where the first correlation ends and the second continues unperturbed. This occurs

at the two prominent lines at $\sim 25\,130.90$ cm^{-1}, which leads to the proposed $D_0 = 25\,130.92$ cm^{-1} for the $^{16}O^{14}N^{18}O$ isotopologue.

There is some uncertainty in this proposed D_0 value because of the sparseness of the line density between 25 130.3 and 25 130.92 cm^{-1}. The absence of strong fluorescence lines over such a relatively significant energy range was not observed in the spectra of the other NO$_2$ isotopologues. The LIF experiment using the $^{16}O^{14}N^{18}O$ gas was reanalyzed after addition of varying amounts of $^{14}N^{16}O_2$ in order to change the relative ratio of the symmetric to asymmetric species. In the sparse region, we observed at least eight weak fluorescence times that could be attributed to the $^{16}O^{14}N^{18}O$ isotopologue including the two prominent ones near 25 130.90 cm^{-1}. Therefore, 25 130.92 cm^{-1} is the established D_0 value for the $^{16}O^{14}N^{18}O$ isotopologue. The asymmetric isotopologues are unique in that they possess two differing dissociation limits, one corresponding to the separation of the ^{16}O atom from $^{14}N^{18}O$ and the other to the separation of the ^{18}O atom from $^{14}N^{16}O$. For asymmetric $^{16}O^{14}N^{18}O$, this second dissociation channel is expected at 25 155.87 cm^{-1} (24.95 cm^{-1} above the first dissociation channel) and at 25 169.21 cm^{-1} for the $^{16}O^{15}N^{18}O$ asymmetric isotopologue (25.35 cm^{-1} above the first dissociation channel; see below). These two differences, 24.95 and 25.35 cm^{-1}, are the differences between the ZPE of $^{14}N^{16}O$ and $^{14}N^{18}O$ and between $^{15}N^{16}O$ and $^{15}N^{18}O$, respectively. Here the question regarding the differences in quantum mechanical properties between symmetric and asymmetric isotopomers arises. Recent theoretical work suggesting an extended predissociation lifetime (longer lifetime) for asymmetric molecules relative to their symmetric counterparts opens the possibility for long lived resonances above D_0 that are capable of fluorescence.[29,9,10] For the main $^{14}N^{16}O_2$ symmetric isotopologue, estimates on the fluorescence lifetime ($\sim 10^{-6}$ s) relative to dissociation lifetime (few 10^{-10} s) suggest that dissociation occurs $\sim 10^3 - 10^4$ time faster than fluorescence, resulting in negligible fluorescence. However, the expected lifetime fluctuations are very large[30] and resonance with long lifetime above D_0 (i.e., with significant radiative probability) cannot be fully excluded for asymmetric isotopologues.

The same energy and intensity correlations were observed in the scrambled NO$_2$ gas containing the ^{15}N isotope. The global decrease in intensity and constant energy correlations between the mixed and pure gases at 25 143.86 cm^{-1} is thus assigned to dissociation of $^{16}O^{15}N^{18}O$ into $^{16}O + ^{15}N^{18}O$. The same technique was used to differentiate $^{15}N^{16}O_2$ fluorescence lines from those of $^{16}O^{15}N^{18}O$ and led to the previous assignment of the $^{15}N^{16}O_2$'s D_0 at 25 141.50 cm^{-1}.

IV. ISOTOPIC EFFECTS ON DISSOCIATION ENERGIES AND THEIR RELATION TO ZERO POINT ENERGIES

Within the BO approximation, the isotopologue dependence of D_0, the dissociation threshold of the NO$_2 + h\nu \rightarrow NO(^2\Pi_{1/2}) + O(^3P_2)$ process is given by

$$D_0(NO_2) = D_e + ZPE_{NO} - ZPE_{NO_2}. \quad (1)$$

In Eq. (1), D_0 and ZPE_{NO_2} are specific to each NO$_2$ isotopologue and ZPE_{NO} specific to each possible NO dissociation product, while D_e is assumed to be the same for all NO$_2$ isotopologues. The precise D_0 values of the six NO$_2$ isotopologues given above are used to confirm the validity of Eq. (1), which is based on the Born-Oppenheimer approximation, by determining if the D_e are constant for each of the NO$_2$ isotopologues. The BO approximation is often tested by assuming theoretical or semiempirical potential energy models and comparing predicted vibrational bands with those observed via high-resolution spectroscopy. For example, isotopologues of water largely agree with the BO approximation; however improved data fits were obtained by including various non-BO corrections.[31] It has also been shown that at low energies O$_3$ also closely follows the BO approximation,[32] but whether this holds at higher energies is not known because the D_0 of O$_3$ cannot be measured at spectroscopic accuracy. In addition, nonspectroscopic methods for determining D_0 have uncertainties that are large relative to the ΔD_0 (~ 10 cm^{-1}), e.g., on the order of $\pm 0.02 - 0.05$ eV (160–400 cm^{-1}) for ozone.[33] Additional difficulties arise from the presence of conical intersections, where excited vibrational states occur on multiple electronic surfaces and are known to cause a breakdown in the BO approximation. Using Eq. (1) and the precise D_0 energies allows for a stringent test of the BO approximation at high energies. Once Eq. (1) is validated, it can be used to predict D_0 for the other isotopologues of NO$_2$ that contain the ^{17}O isotope.

The ZPE_{NO} can be expressed by a Dunham expansion: $G(0) = 1/2\,\omega_e + 1/4\,\omega_e x_e + 1/8\,\omega_e y_e + \cdots$. The ω_e, $\omega_e x_e$, and $\omega_e y_e$ (the zero order frequencies and anharmonic constants) for the main isotopologues of NO have been previously analyzed spectroscopically[34,35] and the corresponding ZPEs are given in Table I. The ω_e^*, $\omega_e x_e^*$, and $\omega_e y_e^*$ for the NO isotopologues [where $*$ denotes the rare (heavy) isotopologues] can also be calculated from the main isotopologue values and utilization of the powers of the square root of the reduced mass ratio.[1] Globally, the relative values of NO ZPEs may be estimated to within a few 10^{-2} cm^{-1} and these uncertainties may be neglected because they are much lower than the errors on ZPE of NO$_2$ isotopologues, which are discussed below.

The ZPE for each NO$_2$ isotopologue can be obtained either by methods using PESs (ZPE$_{CPT}$ see below) or from experimental results using the Dunham expansion (ZPE$_{Dun}$), which for polyatomics without degenerate mode is

$$ZPE_{Dun} = G(0,0,0) = \frac{1}{2}\sum_i \omega_i + \frac{1}{4}\sum_{i \leq j} x_{ij} + \frac{1}{8}\sum_{i \leq j \leq k} y_{ijk}$$

$$+ \frac{1}{16}\sum_{i \leq j \leq k \leq l} z_{ijkl} + \cdots. \quad (2)$$

Here x_{ij}, y_{ijk}, and z_{ijkl} are the anharmonicity constants determined from a fit of experimental vibrational energy levels. For triatomic molecules, each isotopologue has its own set of three normal harmonic frequencies ω_i, which can be calculated using the GF matrix method detailed by Wilson,

Decius, and Cross.[36] Note that the GF matrix method requires four force constants for nonlinear ABA molecules and does not consider anharmonicities. Unknown isotopologues anharmonic constants can be estimated from the empirical relations:[37]

$$x_{ij}^* = x_{ij} \frac{\omega_i^* \omega_j^*}{\omega_i \omega_j}, \quad y_{ijk}^* = y_{ijk} \frac{\omega_i^* \omega_j^* \omega_k^*}{\omega_i \omega_j \omega_k}. \quad (3)$$

Here $*$ denotes the Dunham parameters of the minor isotopologue.

Experimentally only the main isotopologue ($^{14}N^{16}O_2$) and two of the minor NO_2 isotopologues ($^{15}N^{16}O_2$ and $^{14}N^{18}O_2$) have been studied in the IR to evaluate various vibrational frequencies.[38–40] These data are, however, too sparse to enable a proper determination of the Dunham parameters. In contrast, using the laser induced dispersive fluorescence spectrum (LIDFS) technique, Jost and co-workers have observed about 300 vibrational levels of the $^{14}N^{16}O_2$ isotopologue.[41] Combined with previous IR measurements the Dunham expansion up to the z_{ijkl} coefficients have been determined.[41,42] A comparison of various sets of Dunham parameters exhibits significant differences due to the fact the various Dunham parameters are not independent, but depend instead on the maximum order (up to x_{ij} or to y_{ijk} or to z_{ijkl} or to $\cdots$) and on the set of fitted levels (see Table V of Ref. 41). The Dunham parameters also depend on how the $^2B_2$ potential is taken into account.[42] For the purpose of determining the ZPE of $^{14}N^{16}O_2$ the preferred set of Dunham parameters is that of the first column of Table V of Ref. 41, from which ZPE($^{14}N^{16}O_2$) = 1871.05 cm^{-1} is obtained. The $^{14}N^{16}O_2$ ZPE was evaluated for stability (±2 cm^{-1}) by varying the set of fitted levels (from 25 to 75) and the number of Dunham parameters (from 9 to 23). For example, when the NO_2 levels are fitted with a Dunham expansion up to x_{ij} only, the ZPE of $^{14}N^{16}O_2$ is evaluated to be 1872.87 cm^{-1}, 1.82 cm^{-1} higher than that obtained using the Dunham expansion up to y_{ijk}. In contrast, the contribution of the y_{ijk} terms to the ZPE (from a global fit) is only 0.25 cm^{-1}. The D_e values calculated using the precise D_0 energies and the ZPE$_{Dun}$ calculations [Eqs. (2) and (3) and GF matrix] above are given in Table I. It is noteworthy that the ΔZPE$_{Dun}$ are nearly additive, e.g., ΔZPE(848) is close to 2ΔZPE(846), or ΔZPE(858) is close to ΔZPE(848)+ΔZPE(656).

V. DETERMINATION OF ZPE FROM CANONICAL PERTURBATION THEORY

The ZPEs of NO_2 isotopologues were also calculated by applying canonical perturbation theory [23](ZPE$_{CPT}$) to the PESs of Hardwick and Brand[43] (Table I), Tashkun and Jansen,[44] and Schryber et al.[45] Briefly, the PESs and the kinetic energy operators are first Taylor-expanded around the minimum of the PES, and the GF matrix method[36] is applied in order to express the resulting polynome in terms of the dimensionless normal coordinates. A series of canonical (or unitary) transformations is then performed in order to rewrite the Hamiltonian of the system in terms of as complete as possible a set of good quantum numbers. For NO_2, the transformed Hamiltonian thus depends uniquely on the three good

quantum numbers for symmetric stretch, bend, and antisymmetric stretch, respectively, and the energies of the system are just obtained as a polynomial function of these quantum numbers [see, for example, Eq. (2) for the energy of the ground state]. This is also the case for SO_2. In contrast, in the case of O_3, the symmetric and antisymmetric stretches are coupled by a 1:1 Darling-Dennison resonance, while in the case of CO_2 the symmetric stretch and the bend are coupled by a 2:1 Fermi resonance. These resonances must be taken into account in the canonical transformations, so that one quantum number is lost for O_3 and CO_2. Since the ground state is not coupled to any other state, this has, however, no influence on the calculation of its energy, which is still obtained from the evaluation of an expression of the form of Eq. (2).

The ZPE$_{CPT}$ obtained by applying CPT to the quartic PES of Hardwick and Brand[43] are similar to ZPE$_{Dun}$, but are systematically larger by about 3 cm^{-1} (2.88 cm^{-1} on average), while the ZPE$_{CPT}$ obtained from the PES of Tashkun and Jansen[44] are systematically larger by about 6 cm^{-1} compared with ZPE$_{Dun}$. This latter PES has been designed to reproduce a large number of high lying vibrational levels, at the cost of a less accurate description of the bottom of the PES. The same arguments hold for the PES of Schryber et al.,[45] while the recent ab initio PES of Kurkal, Fleurat-Lessard, and Schinke[46] results in still much higher ZPEs, because it was not adjusted against experimental energies as the three former PES.[43–45] Therefore only the ZPE$_{CPT}$ from the PES by Hardwick and Brand PES (Ref. 43) are considered below.

At this point, two comments are in order. First, the accuracy of CPT results are limited by the quality of the PES. Errors in the PES are, however, systematic ones, in the sense that they are essentially independent of the isotopologue under consideration. Therefore, these errors are almost not reflected in the computed isotopic energy shifts. This implies that the isotopic energy shifts are computed with a much higher accuracy than the energies of the ground states themselves. The second remark deals with the fact that the kinetic energy operator, which is used in CPT calculations, is an approximate one. For example, the so-called potential-like kinetic term, which arises from the nonlinear relationships between Cartesian and valence or Jacobi coordinates, is not taken into account. This results in an additional error in the computed ground state energies, which can reach a few cm^{-1}. Again, this error is essentially systematic (i.e., almost isotopologue independent), so that it affects only very weakly the computed isotopic energy shifts.

For NO_2, these arguments lead us to use rescaled ZPEs, defined as ZPE$_{CPT-Resc}$ = 0.998 393ZPE$_{CPT}$ for the determination of D_e, instead of ZPE$_{Dun}$. The scaling factor 0.998 393 is the ratio ZPE$_{Dun}$(646)/ZPE$_{CPT}$(646), which rescales ZPE$_{CPT}$ with respect to ZPE$_{Dun}$ for the 646 isotopologue, the only isotopologue for which precise experimental vibrational energies (and thus ZPE$_{Dun}$) are known. The ZPE$_{CPT-Resc}$ are listed in Table I and used to determine the "best" set of D_e values, and the initial ZPE$_{CPT}$ and ΔZPE$_{CPT}$ (not rescaled) can be found in Table II.

It should be noted that even if the ZPE$_{CPT}$ are systemati-

TABLE II. The zero point energies of the main isomers of oxygen symmetric triatomics and the ΔZPE of their isotopomers/isotopologues as calculated by CPT. NO_2 surface (Ref. 43) (Dunham expansion, sixth-order CPT). O_3 surface (Ref. 32) (Dunham expansion+Darling-Dennison resonance, sixth-order CPT). SO_2 surface: (VQZ+1) (Ref. 47) (Dunham expansion, sixth-order CPT). CO_2 surface (Ref. 48) (Dunham expansion+Fermi resonance, sixth-order CPT).

Central atom X		Terminal oxygen atom pair					
		ΔZPE symmetric isotopomers			ΔZPE asymmetric isotopomers		
		$^{16}OX\,^{16}O$	$^{17}OX\,^{17}O$	$^{18}OX\,^{18}O$	$^{16}OX\,^{17}O$	$^{16}OX\,^{18}O$	$^{17}OX\,^{18}O$
NO_2	^{14}N	1874.06	28.75	54.71	14.33	27.18	41.69
	^{15}N	30.04	59.11	85.36	44.52	57.51	72.19
O_3	^{16}O	1450.00	23.22	44.21	11.16	20.75	33.33
	^{17}O	19.68	42.99	64.19	30.82	40.52	53.21
	^{18}O	37.13	60.85	82.21	48.53	58.35	71.15
SO_2	^{32}S	1529.82	30.78	58.62	15.35	29.17	44.67
	^{33}S	7.48	38.39	66.35	22.90	36.78	52.34
	^{34}S	14.55	45.59	73.66	30.03	43.96	59.59
	^{36}S	27.68	58.95	87.24	43.27	57.30	73.06
CO_2	^{12}C	2533.85	35.01	66.62	17.47	33.16	50.78
	^{13}C	52.73	88.19	120.21	70.42	86.32	104.16
	^{14}C	99.01	134.89	167.30	116.91	133.01	151.06

cally larger than $\mathrm{ZPE_{Dun}}$, the isotopologue *shifts*, $\mathrm{\Delta ZPE_{CPT}}$ and $\mathrm{\Delta ZPE_{CPT\text{-}Resc}}$ are close to the shifts obtained from $\mathrm{ZPE_{Dun}}$, with a largest difference of only 0.25 and 0.20 cm^{-1}, respectively. The 1.6 cm^{-1} difference in D_e relative to determination of Jost *et al.* at 26 049.36 cm^{-1} (see Ref. 18) is mainly due to the ZPE of $^{14}N^{16}O_2$, ZPE being taken at 1869.45 cm^{-1} in Ref. 18, instead of the 1871.05 cm^{-1} value used here. The small differences between the six D_e (see the two last lines of Table I) may be tentatively interpreted in terms of two small systematic errors in $\mathrm{\Delta ZPE_{CPT\text{-}Resc}}$. The first one is an overestimation of 0.22 cm^{-1} for a ^{16}O to ^{18}O substitution. The second is an underestimation of 0.16 cm^{-1} for a ^{14}N to ^{15}N substitution. Assuming the ΔZPE is additive upon isotopic substitution, these two corrections applied to the five isotopologues [(646) is used as reference] lead to six values for D_e, which are very close $\langle D_e \rangle = 26051.07$

FIG. 5. A comparison of ΔZPE calculated by the CPT method compared with those derived from available experimental data for CO_2 (●) (Ref. 2), O_3 (■) (Ref. 53), (♦) (Ref. 52), NO_2 (□) (Refs. 38 and 39), SO_2 (▲) (Refs. 50 and 51) using either zero-order frequencies and Dunham expansions (Refs. 2, 38, 39, and 50–52) or fundamental vibrations (Ref. 52). Numeric notation indicates the isotopologue configuration, for example 668=$^{16}O^{16}O^{18}O$.

± 0.06 cm^{-1}. This dispersion is close to the experimental uncertainty (±0.05 cm^{-1}) on the measured D_0. These results reinforce the validity of the BO approximation, though some minute systematic non-BO energy contributions cannot be excluded.

These results show that the isotopologue shifts of ZPEs, ΔZPE, determined by CPT calculations are precise to within a fraction of a cm^{-1}. Given the confirmed accuracy of the CPT method for the isotopologues of NO_2, we next used the same method to determine the ΔZPE for three molecules, which are important in atmospheric chemistry, namely, O_3, SO_2, and CO_2. Results can be found in Table II. The recent surfaces of Tyuterev *et al.*[32] for ozone, of Martin[47] for SO_2, and of Zuniga *et al.*[48] for CO_2 were used in CPT calculations. These calculated ΔZPEs are compared with previous experimental determination, available in Fig. 5. There is an overall good agreement between CPT calculations and spectroscopic data, with differences usually smaller than 1 cm^{-1}. CPT calculations thus provide precise ΔZPE for triatomic molecules where no spectroscopic data are available.

VI. CONCLUSIONS

Using jet cooled conditions and LIF techniques the dissociation energies of six isotopologues of NO_2 have been determined. These energies (in cm^{-1}) are

$$25\,128.56\,(^{14}N^{16}O_2), \quad 25\,141.50\,(^{15}N^{16}O_2),$$
$$25\,158.70\,(^{14}N^{18}O_2), \quad 25\,171.80\,(^{15}N^{18}O_2),$$
$$25\,143.86\,(^{16}O^{15}N^{18}O), \quad 25\,130.92\,(^{16}O^{14}N^{18}O)$$

with a precision better than ±0.05 cm^{-1}. A common $\langle D_0 \rangle = 26\,051.22$ cm^{-1} with a maximum deviation of ±0.33 cm^{-1} is derived using calculated ZPEs. This small dispersion of D_e suggests that the BO approximation is valid for this problem. Tentatively, an even better agreement can be obtained by applying two empirical corrections, which reduce the dispersion in D_e estimations to the experimental uncer-
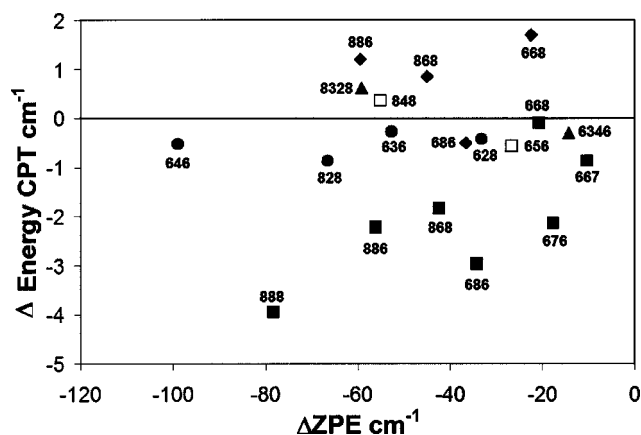
tainty of ± 0.05 cm^{-1}. Note that these corrections will be confirmed in the future by the measurement of the vibrational energy levels of various isotopologues of NO$_2$.

Moreover, the agreement between experimental results and canonical perturbation theory calculations shows that this method can be used to determine the ΔZPE for a variety of oxygen symmetric triatomic molecules. These precise values can be used to determine isotopic fractionation factors arising from a ΔZPE in chemical and photochemical reactions as well as constraints on expected fractionations in isotopic models.

[1] G. Herzberg, *Infrared and Raman Spectra of Polyatomic Molecules* (Van Nostrand, New York, 1966).

[2] H. C. Urey, J. Chem. Soc. **1947**, 562.

[3] J. Bigeleisen and M. G. Mayer, J. Chem. Phys. **15**, 261 (1947).

[4] J. Hoefs, *Stable Isotope Geochemistry* (Springer, Berlin, 1973).

[5] C. E. Miller and Y. Yung, J. Geophys. Res. **105**, 29 (2000).

[6] Y. L. Yung and C. E. Miller, Science **278**, 1778 (1997).

[7] Y. Q. Gao and R. A. Marcus, Science **293**, 259 (2001).

[8] B. C. Hathorn and R. A. Marcus, J. Chem. Phys. **111**, 4087 (1999).

[9] D. Babikov, B. K. Kendrick, R. B. Walker, R. T Pack, P. Fleurat-Lesard, and R. Schinke, J. Chem. Phys. **119**, 2577 (2003).

[10] D. Babikov, B. K. Kendrick, R. B. Walker, R. Schinke, and R. T Pack, Chem. Phys. Lett. **372**, 686 (2003).

[11] E. D. Young, A. Galy, and H. Nagahara, Geochim. Cosmochim. Acta **66**, 1095 (2002).

[12] R. A. Marcus and Y. Q. Gao, J. Chem. Phys. **114**, 9807 (2001).

[13] J. A. Kaye, J. Geophys. Res. **91**, 7865 (1986).

[14] M. H. Thiemens, J. Savarino, J. Farquhar, and H. Bao, Acc. Chem. Res. **34**, 645 (2001).

[15] K. Mauersberger, D. Krankowsky, and C. Janssen, Space Sci. Rev. **106**, 265 (2003).

[16] J. A. Kaye and D. F. Strobel, J. Geophys. Res. **88**, 8447 (1983).

[17] G. Michalski, Z. Scott, M. Kabiling, and M. Thiemens, Geophys. Res. Lett. **30**, ASC 14-1 (2003).

[18] R. Jost, J. Nygard, A. Pasinski, and A. Delon, J. Chem. Phys. **105**, 1287 (1996).

[19] J. Miyawaki, K. Yamanouchi, and S. Tsuchiya, J. Chem. Phys. **99**, 254 (1993).

[20] R. E. Smalley, L. Wharton, and D. H. Levy, J. Chem. Phys. **63**, 4977 (1975).

[21] A. Delon and R. Jost, J. Chem. Phys. **110**, 4300 (1999).

[22] A. Delon, R. Jost, and M. Lombardi, J. Chem. Phys. **95**, 5701 (1991).

[23] M. Joyeux and D. Sugny, Can. J. Phys. **80**, 1459 (2002).

[24] R. Georges, A. Delon, and R. Jost, J. Chem. Phys. **103**, 1732 (1995).

[25] J. Miyawaki, K. Yamanouchi, and S. Tsuchiya, Chem. Phys. Lett. **180**, 287 (1991).

[26] J. C. D. Brand, W. H. Chan, and J. L. Hardwick, J. Mol. Spectrosc. **56**, 309 (1975).

[27] K. Yamanouchi, S. Takeuchi, and S. Tsuchiya, Prog. Theor. Phys. Suppl. **98**, 420 (1989).

[28] G. Persch, H. J. Vedder, and W. Demtroeder, J. Mol. Spectrosc. **123**, 356 (1987).

[29] D. Babikov, B. K. Kendrick, R. B. Walker, R. T Pack, P. Fleurat-Lessard, and R. Schinke, J. Chem. Phys. **118**, 6298 (2003).

[30] B. Kirmse, B. Abel, D. Schwarzer, S. Y. Grebenshchikov, and R. Schinke, J. Phys. Chem. A **104**, 10398 (2000).

[31] H. Partridge and D. W. Schwenke, J. Chem. Phys. **106**, 4618 (1997).

[32] V. G. Tyuterev, S. Tashkun, P. Jensen, A. Barbe, and T. Cours, J. Mol. Spectrosc. **198**, 57 (1999).

[33] M. Allan, K. R. Asmis, D. B. Popovic, M. Stepanovic, N. J. Mason, and J. A. Davies, J. Phys. B **29**, 3487 (1996).

[34] J. L. Teffo, A. Henry, P. Cardinet, and A. Valentin, J. Mol. Spectrosc. **82**, 348 (1980).

[35] A. Henry, M. F. Lemoal, P. Cardinet, and A. Valentin, J. Mol. Spectrosc. **70**, 18 (1978).

[36] E. B. Wilson, J. C. Decius, and P. C. Cross, *Molecular Vibrations; the Theory of Infrared and Raman Vibration* (McGraw-Hill, New York, 1955).

[37] G. Herzberg, *Spectra of Diatomic Molecules* (Van Nostrand, New York, 1966).

[38] M. D. Olman and C. D. Hause, J. Mol. Spectrosc. **26**, 241 (1968).

[39] R. E. Blank and C. D. Hause, J. Mol. Spectrosc. **34**, 478 (1970).

[40] E. T. Arakawa and A. H. Nielsen, J. Mol. Spectrosc. **2**, 413 (1958).

[41] A. Delon, R. Jost, and M. Lombardi, J. Chem. Phys. **95**, 5701 (1991).

[42] M. Joyeux, R. Jost, and M. Lombardi, J. Chem. Phys. **119**, 5923 (2003).

[43] J. L. Hardwick and J. C. D. Brand, Chem. Phys. Lett. **21**, 458 (1973).

[44] S. A. Tashkun and P. Jensen, J. Mol. Spectrosc. **165**, 173 (1994).

[45] J. H. Schryber, O. L. Polyansky, P. Jensen, and J. Tennyson, J. Mol. Spectrosc. **185**, 234 (1997).

[46] V. Kurkal, P. Fleurat-Lessard, and R. Schinke, J. Chem. Phys. **119**, 1489 (2003).

[47] J. M. L. Martin, J. Chem. Phys. **108**, 2791 (1998).

[48] J. Zuniga, A. Bastida, M. Alacid, and A. Requena, J. Mol. Spectrosc. **205**, 62 (2001).

[49] M. De Hemptinne, R. Van Riet, A. Defossez, F. Bruyninck, and P. Dachhelet, Ann. Soc. Sci. Bruxelles, Ser. 1 **77**, 163 (1963).

[50] R. van Riet, Ann. Soc. Sci. Bruxelles, Ser. 1 **78**, 237 (1964).

[51] V. G. Tyuterev, S. A. Tashkun, D. W. Schwenke, and A. Barbe, Proc. SPIE **5311**, 176 (2003).

[52] B. C. Hathorn and R. A. Marcus, J. Phys. Chem. **105**, 5586 (2001).